20

Ti indiffused Lithium Niobate (Ti: $LiNbO_3$) Mach-Zehnder interferometer all optical switches: A review

G.Singh, R.P.Yadav and V.Janyani
Department of Electronics & Communication Engineering
Malaviya National Institute of Technology Jaipur-India
E-mail: gschoudhary75@gmail.com

1. Introduction

Appropriate switching technology plays a major role in deciding the workable layout of any network and can improve accuracy, speed, scalability and flexibility efficiently, if chosen and implemented in best possible way. All-optical switches (O-O-O) do not require opto-electronic conversion and regeneration steps, as in case of mixed switches (O-E-O), where switching is done in electronic form. The development of all optical switches becomes necessary to fit them with the fast networks to make use of WDM technology, which incorporates hundreds of wavelength channels over a single fiber link. The speed and sensitivity of optical switches necessarily has to match with new generation photonic networks requirement, in which light not only carries the data and routing information, but also controls the switches in its path directly. Various optoelectronic materials, with MMI, MZI and other structures, have been used to design all optical switches like Si, SOI, InP, InP/InGaAsP, InGaAs–AlGaInAs, $LiNbO_3$, photonic crystals etc. InP/lnGaAsP optical integrated MMI switches (Shintaro et al., 2008), InGaAsP-InP MZI optical space switch (Agrawal et al., 1995) and monolithically integrated InGaAs–AlGaInAs machzehnder interferometer optical switch using quantum-well intermixing (Wong et al., 2005) are some of examples. The electro-optic coefficient of lithium niobate is well suited for modulation and switching of fast optical communication systems.

A lithium niobate with a Ti diffused waveguides are useful for optical fiber communication and signal processing. Ti: $LiNbO_3$ technology has been used to fabricate switch/modulators, acousto-optic deflectors, tunable wavelength filters, polarization controllers and splitters, frequency shifters and doublers (Alferness, 1986). The optical loss of a conventional Ti: $LiNbO_3$ waveguide modulator is usually 0.2 dB/cm, and posses a graded index profile (Xiaobo, 2004). Ti diffused LN had also been used to fabricate phase modulators, by placing it in the middle of a travelling wave structure (Binh et al., 2007). The chapter is organized in the following sections. Section 2 summarizes the lithium niobate and Ti diffused lithium niobate material properties and characteristics. Section 3 gives a brief introduction to all optical switches and their advantages for using them with fast communication systems and networks. Section 4; explain the principle of operation of MZI based switches and their applications. In Section 5, the design of all optical switches using MZI structures on Ti doped lithium niobate are elaborated. This section also discusses the effect of other parameters on the performance of the designed switch. Section 6 contains the discussion and concluding remarks.

2. Lithium Niobate- A crystal for optical processing

Lithium Niobate ($LiNbO_3$) is a colorless, insoluble with water and ferroelectric material suitable for a variety of applications. Its electro-optical, acousto-optical and non linear optical properties attract designers to use it in integrated optics and have been proved as excellent material for optical waveguides manufacturing. The property of high intrinsic modulation bandwidth makes it a suitable candidate for communication technology. Table 1 gives list of various specifications for lithium niobate crystal (courtesy: Almaz optics, Inc.). The lithium niobate is a versatile material & used for various applications in guided wave optics, electro-optics, acousto-optics and nonlinear optics.

Chemical Formula	$LiNbO_3$
Crystal Class	Trigonal, 3m
Solubility in water	None
Color	None
Molecular Weight	147.9
Density, g/cm^3 at 293 K	4.644
Transmittance Range, nm	350-5500
Dielectric Constant at 100 KHz e_a (perpendicular), e_c (parallel)	85, 29
Melting Temperature, K	1530
Curie Temperature, K	1415
Thermal Conductivity, W/(m K) at 300 K	5.6
Bandgap, eV	4.0
Optical Damage Threshold at 1064 nm, t ~ 10 nsec, MW/cm^2	250

Table 1. $LiNbO_3$ crystal spec. (courtesy: almaz optics, Inc.)

Its piezo-electric and photo-elastic properties had been used for various technical developments. Lithium niobate has been used to fabricate integrated waveguides because of its high electro-optic coefficient, optical damage resistance and low losses (Kalabin et al., 2004). Their Strain-optic effects are used to implement wavelength-tunable polarization converters (Wang & Chung, 2004). The use of $LiNbO_3$ modulators, with bulky diode pumped YAG lasers and cavity RF filters to construct Optoelectronic oscillators (OEO's) with ultra-low phase noise capability is explained by (Yao & Maleki, 1999). The use of lithium niobate to make QPM structure by reversing the spontaneous polarization under the influence of a sufficiently large electric field has been reported in (Xiuping, 2006). The lithium niobate material has been extensively used to design switches with low loss, but their polarization dependency is the major concern (Suzuki et al., 2008). The choice of LN based switches is proved as best for high and low speed systems (Thylen, 1989). In recent years, $LiNbO_3$ devices have successfully addressed the modulation requirements in digital fiber-optic time-domain-multiplexed (TDM) and wavelength-division-multiplexed (WDM) systems (Wooten et al., 2000).

2.1 Ti-diffused Lithium Niobate

$LiNbO_3$ waveguides can be fabricated to design switches and modulators using either titanium in-diffusion or annealed proton exchange processes. To fabricate planner waveguides, the entire $LiNbO_3$ is subjected to while for channel waveguides, photolithography process is used to defined masks for selected regions on it with these processes. In some cases, Mg oxide is doped with $LiNbO_3$ to control optical damages. The proton-exchanged lithium niobate waveguides is easy to fabricate and can operate with low temperature. Ti diffused lithium niobate waveguides are useful for various communication, signal processing and sensor systems. Ti doping in the lithium niobate crystal increases refraction indexes, and which allow both TE and TM modes to propagate along the waveguides, which satisfies desired conditions for optical signal processing.

3. All optical switches

An optical switch routes an optical signal from one or more input ports to one or more output ports. Theoretically, all optical switches (O-O-O) are independent of bit rate and protocols with unlimited scalability, which leads to more flexibility in the network. The choice of technology, switch architectures and size as well, plays an important role in performance of all optical switches. Following figure 1 shows a basic all optical switch with two different possible switching states named as bar & cross state. In this, inputs & outputs are in optical form and the switching is also performed in optical domain within the device.

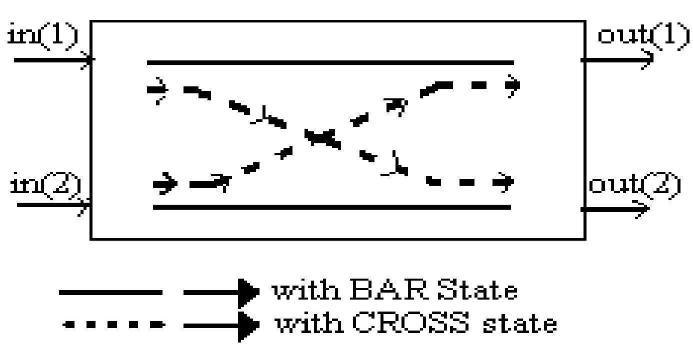

Fig. 1. All optical switch

The use of all optical switches are now taking over the use of O-E-O switches, as the O-E-O switches requires complex circuitry and have their own limitation while performing smooth & lossless switching. The most common applications of these are WDM optical add–drop multiplexing (OADM), cross connects and protection switching. Yet the use of all optical switches are to cover up O-E-O switches uses in optical switching because of their difficulty in accommodating within the circuit with the use of VLSI technology, while fabrication with low fabric losses and to use the same to realize higher order switches.

4. MZI structures & their switching behavior

Among different topologies, MZI structures are most efficient, converts a phase modulation into an intensity modulation, which is widely used for many optical applications e.g. modulators etc. Monolithically integrated MZI switches represent the most promising solution due to their compact size, thermal stability and low power (few fJ for input signal and few hundred fJ for control pulse) operation. Basic 2x2 MZI switch structure can be viewed, as shown in figure 2, as two interferometric arms of equal length connecting two –3db couplers. The first coupler is used to split the signals in two beams, which when passed through the interferometric arms experiences phase difference. This phase difference is due to voltage variations across electrodes covering interferometric arms that in turn changes refractive indices. Finally, both the beam with different phases are put together again into a single signal by the second -3 db coupler, and the outputs are observed as per constructive or destructive interference (Papadimitriou et al., 2003).

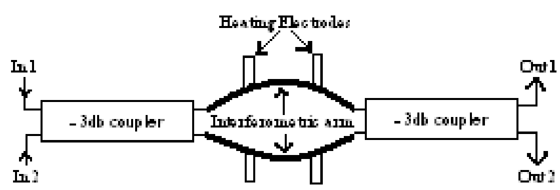

Fig. 2. Basic 2x2 MZI switch structure, ref. [10]

The LN has been used to design modulators and switches based on machzehnder interferometer or directional coupler efficiently. The symmetric machzehnder interferometer (MZI) has shown the better flexibility and shortest switching windows as compared to various configurations (Toliver et al., 2000). Improvement in all optical switching performance and high-speed capability of the MZI switches are investigated in (Schreieck et al., 2001), (Song et al., 2005) respectively. The integration of SOA's with in the MZI structures also the useful technology to design polarization insensitive switches (Gupta et al., 2005). Recently the MZI structures are fabricated using the photonic crystal to achieve the goals of VLSI photonics (Han et al., 2008). The MZI can be configured as an intensity modulator or a switch, but its periodical response can be a drawback since it requires an accurately controlled driving voltage

5. Design of MZI all optical switches

5.1 Design steps:

In this part, we have elaborated the design of Machzehnder interferometer based 2 x 2 all optical switch. Figure 3 shows the switch layout, which has been designed and simulated with the opti bpm layout designer.

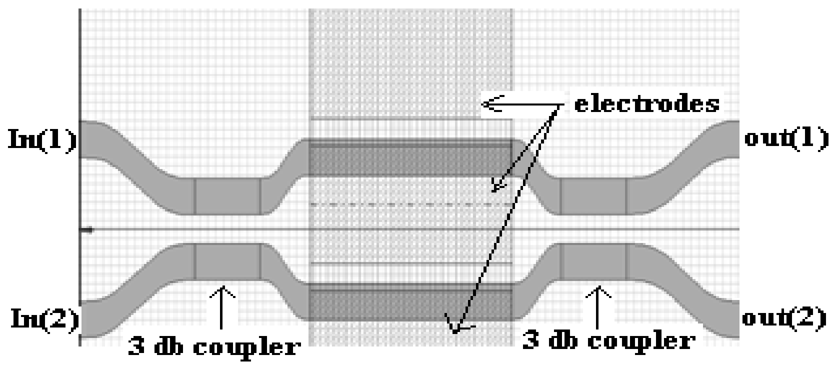

Fig. 3. 2 x 2 MZI switch layout

We assume that the integrated switch is created on a z-cut wafer of Lithium Niobate and is surrounded by air cladding. The device is oriented along Y–optical axis of the Lithium Niobate. Therefore, we define a diffused material for the substrate and a dielectric material for cladding. The crystal lithium niobate has a crystal cut along z axis and propagation direction along y axis. The dielectric material selected is air with refractive index 1.0. Traditionally, $LiNbO_3$ waveguides are fabricated using either titanium in-diffusion or annealed proton exchange processes (APE). The main advantage of proton-exchanged waveguides is the low (approximately 240°C) temperature, less than Curie point, and easy fabrication process (Korkishko et al., 2003). The diffusion of Titanium in Lithium Niobate substrate is being used to design the machzehnder interferometer waveguide. Ti doping in the lithium niobate crystal increases refractive indices, and allow both TE and TM modes to propagate along the waveguides. Only one diffused profile is needed ($TiLiNbO_3$). The insertion losses of the devices can be minimized by controlling the profile of in diffusion process. Using this technique an integrated 1×2 Mach–Zehnder linear analog modulator with 3 dB on chip losses is reported at (Arrioja et al., 2008). Other design parameters used are listed in table 2 and table 3 (courtesy: BPM layout designer, Optiwave Inc.)

Diffused material	*Dielectric material*
Crystal: $LiNbO_3$ Crystal cut: Z Propagation direction: Y	Material: Air Refractive index: 1.00
Diffused profile: Ti $LiNbO_3$ PRO 1	
Waveguide properties	
Wafer profile: Ti $LiNbO_3$ Wafer dimension (all in μ mts) Length =33000, Width = 8.0, Breadth =100	
3D Wafer properties	
Cladding	*Substrate*
Material: Air Thickness (μ mts): 2.0	Material: $LiNbO_3$ Thickness (μ mts): 10.0

Table 2. MZI design Specifications

Electrode 1		Electrode 2		Electrode 3		Gap 1-2	Gap 2-3
W	V	W	V	W	V	W	W
50	0.0	26	0.0	40	0.0	6.0	6.0
50	0.0	26	6.75	40	1.5	6.0	6.0
Electrode 2 center position : 5.5							
Stripe thickness before diffusion						0.05 µm	
Dopant constant						5.67e+022	
Lateral diffusion length(D_H)						4 µm	
Diffusion length in-depth(D_V)						3.5 µm	

Table 3. Specifications for electrode & other regions. {W=width (µ mts) V= voltage (volts)}

5.2 Observations

We checked the RI profile of the XY slice. We also defined an electrode region on the substrate and built up electrodes on the top of a buffer layer. The input plane has been selected with MODE as the starting field and 0.0 as Z –offset. After the input plane has been defined the global data is set with refractive index MODAL and wavelength 1.3 micrometer. We calculated the 2D isotropic simulation. We varied the electrode voltages for region 2. More detailed investigations of the electro-optic switch have been performed using the scripting language. We scanned the voltage on the central electrode and observed the overlap integral of the output ports with the waveguide mode. The switch is found to have better switching from CROSS to BAR state for electrode voltage value in between 6.6 and 6.8 volt with negligible coupling losses. States (cross and bar) of the switch are shown in figure 4 and figure 5 with their corresponding optical field propagation in 3D views.

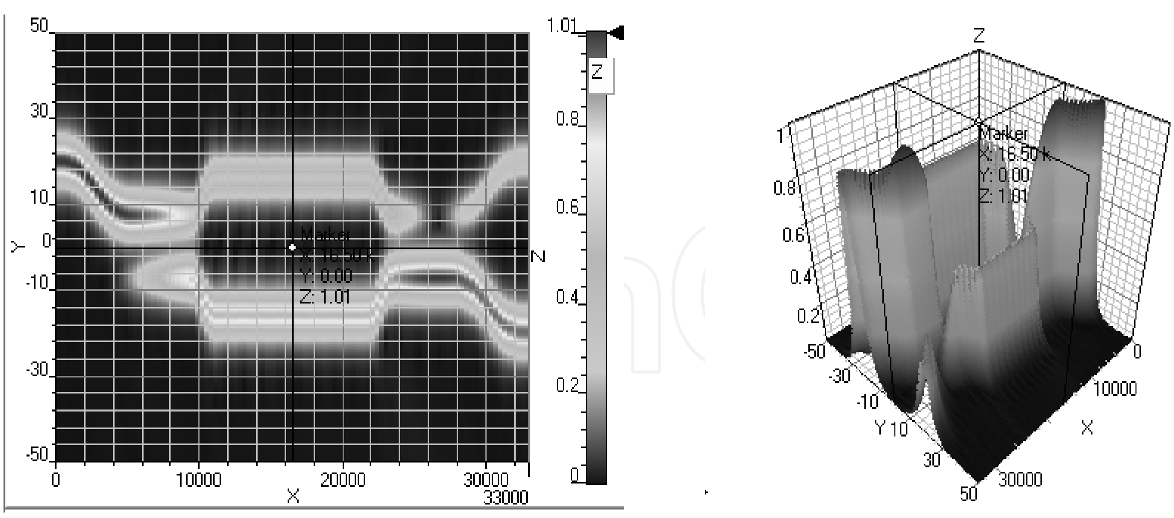

(a) (b)

Fig. 4. (a) Switch with CROSS state (b) Optical field propagation for CROSS state (3D View)

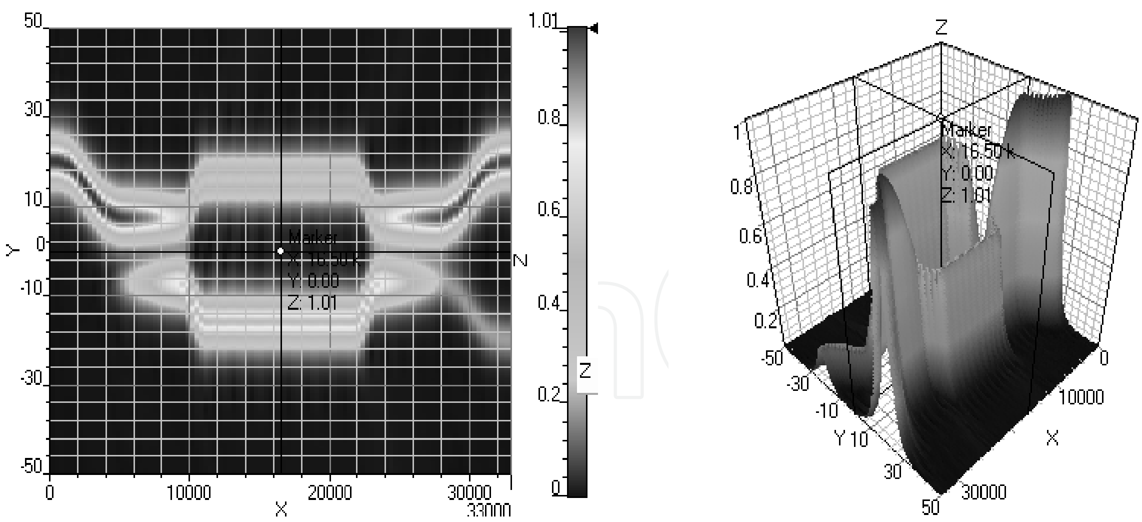

(a) (b)

Fig. 5. (a) Switch with BAR state (b) Optical field propagation for BAR state (3D view)

5.3 Discussion: effects of electrode shape & size:

In this section, we have discussed the effect of electrode dimension especially in terms of its length and spacing with with each other, to perform desired switching for signals with wavelength of 1.3 µm and 1.55 µm. We performed different iterations with changes in the electrode voltages, incrementing it by 0.8 volts per iteration and found the switching voltages for different length of electrode region. For this, we have taken refractive index of the electrode buffer part as 1.47, buffer layer thickness 0.3 µm, horizontal permittivity 4, vertical permittivity 4 and electrode thickness 4 µm. Also, the width of electrodes 1 and 3 is kept at 50 µm initially, while for electrode 2, width is 26 µm & positioned at 5.5, centrally. The electrode gap (spacing) is kept at 6.0 µm initially. Figure 6 indicate the d_1 & d_2, the spacing considered for these effects.

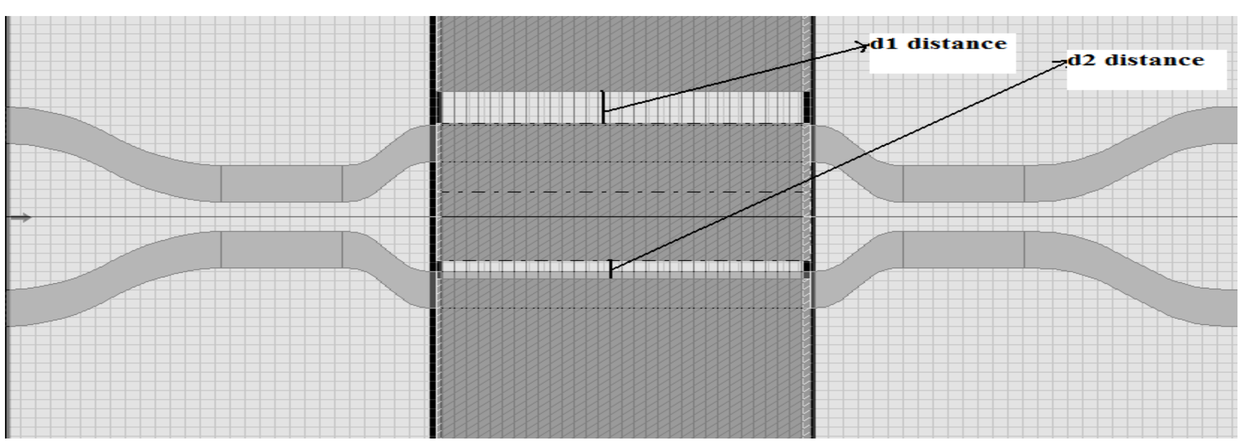

Fig. 6. Layout of the MZI switch with parameters given above.

Observation no:	Electrodes dimension (µm)	Length of the electrode (µm)	Voltage for bar state(V)	Voltage for cross state(V)
1	11500-21500	10000	0	6.75
2	11550-21450	9900	0	9.0

3	11600-21400	9800	0	14
4	11650-21350	9700	0	16
5	11700-21300	9600	0	18.5
6	11750-21250	9500	0	-

Table 4. Electrodes dimension variations & respective switching voltages

From the observation as depicted in table 4, it has been found that when we decrease the length of electrode region the switching voltage for the MZI switch increases, which is required to change its bar state to the cross state and on the further decrease of the electrode region result into distortion of the switching ability. When we decrease it further, it has been found that MZI is not able to perform proper switching at this stage.

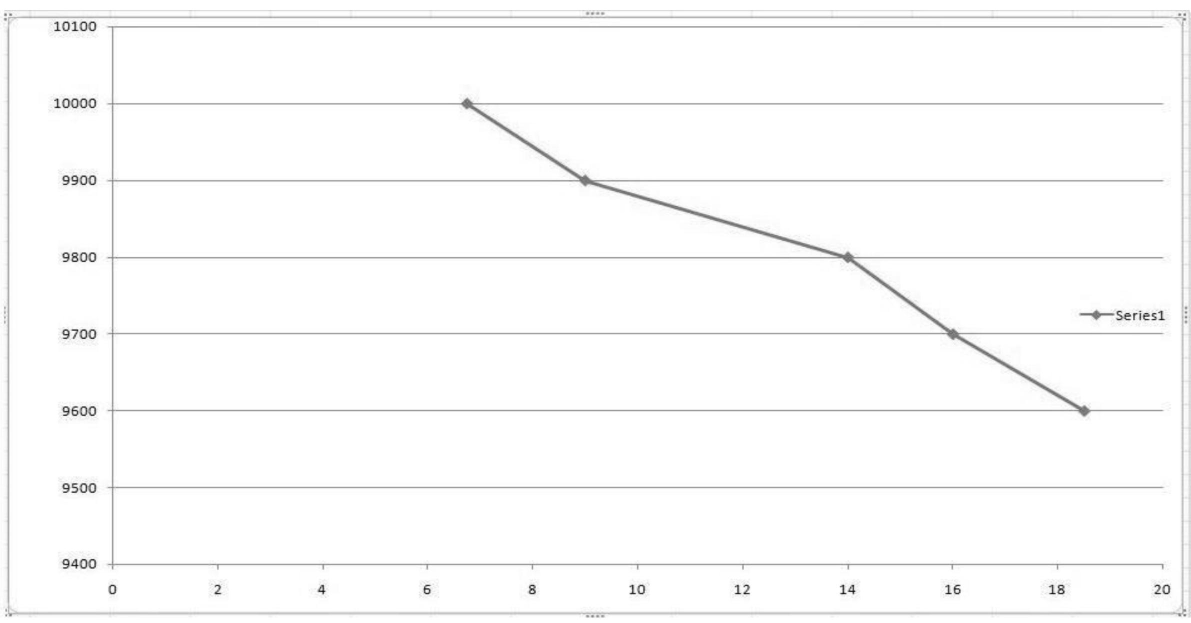

Fig. 7. Switching voltage against the electrode length variations

Following table 5 shows the driving voltage Vs different value of electrodes gap in µm. The driving voltage varies as we change the width of the electrode of the electrode 2. This table shows the effect of the width of the change of the electrode on driving voltage. The effect of electrode length is depicted graphically also, shown in figure 7.

d_1(µm) / d_2 (µm)	1	2	3	4	5	6	7
1	12.5	13.5	14.0	14.0	14.0	14.5	12.0
2	13.5	12.5	13.5	12.5	12.5	12.0	9.50
3	14.0	13.5	12.5	10.5	10.5	10.0	9.25
4	14.5	13.0	10.0	8.80	7.00	8.00	9.00
5	14.5	12.0	11.5	8.75	8.00	8.50	7.50
6	15.0	10.0	11.0	9.50	8.25	6.75	7.75
7	16.0	15.0	14.0	12.0	11.7	11.5	8.00

Table 5. Switching voltage matrix representation w.r.t different values of d_1 and d_2 (electrodes spacing).

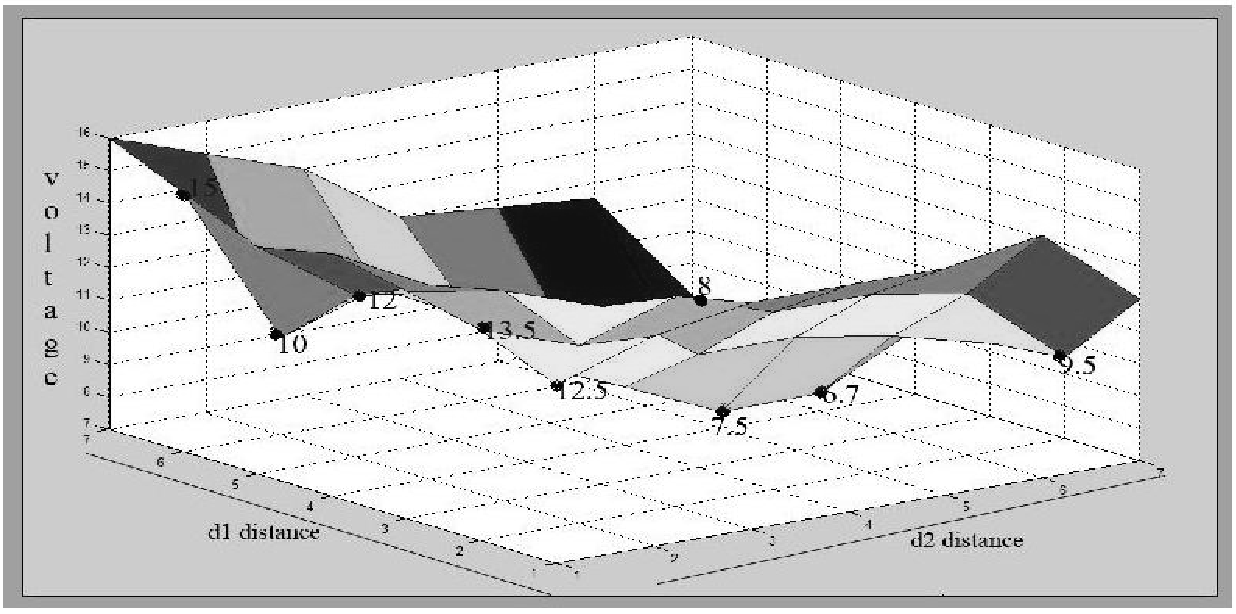

Fig. 8. Graphical (3D view) representation of the switching voltage v/s d_1 & d_2

From table 5 and figure 8 we observed that when the hot electrode is placed exactly on both the waveguide, this results minimum coupling in the MZI arms. Even when one of the gaps between the electrodes is more i.e. when hot electrode isn't on the waveguide then this also results minimum coupling and needs higher voltage for the switching. When the width of the electrode region is changed, the switching voltage also changes depends width and alignments, as shown in figure 8.

Effect of the change of the coupling region of the 3 dB coupler: when we changed the coupling region of the 3dB coupler this results in the distortion in the output of the 1st coupler, as a result of which the characteristics of the MZI switch looses. It can't act as the switch in this condition. Figure 9 and figure 10 shows the effect of variation of electrode voltage with respect to unit output power across bar & cross states and switching in between these states for input signals with wavelength of 1.3 μm and 1.55 μm respectively.

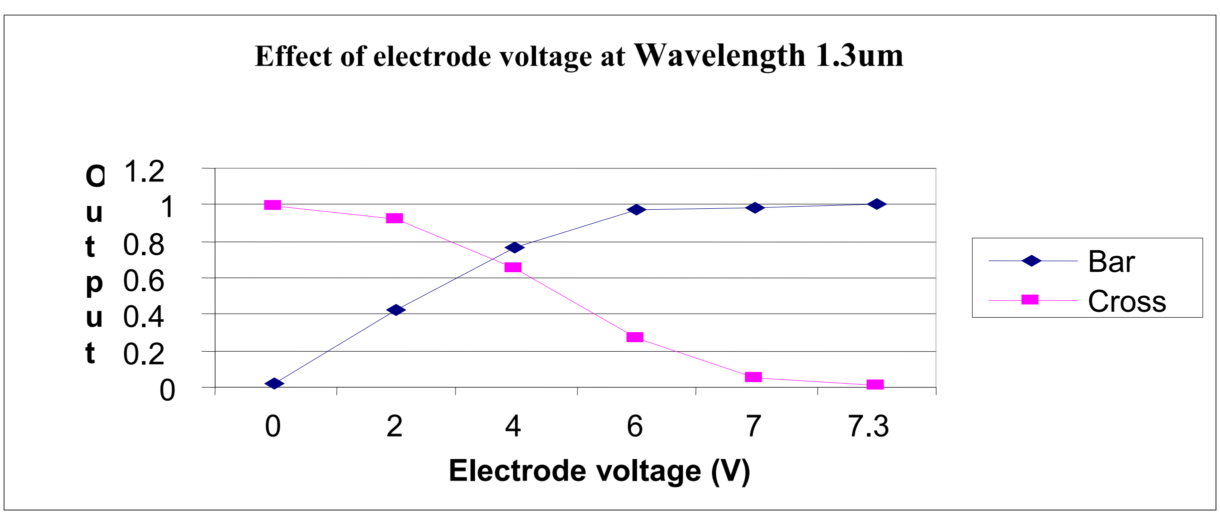

Fig. 9. Variation of output power with electrode voltage (λ=1.3 μm)

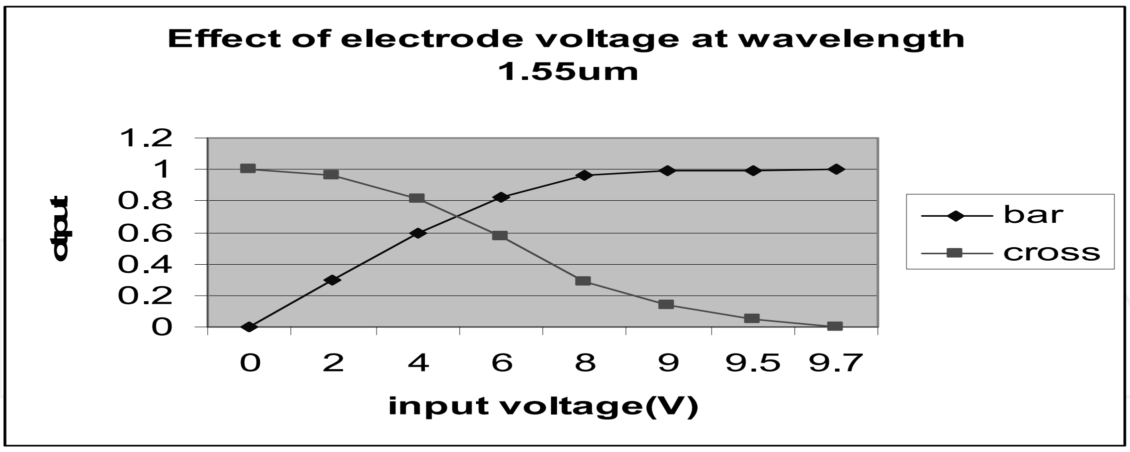

Fig. 10. Variation of output power with electrode voltage (λ=1.55 μm)

6. Conclusion

This chapter reviewed the Machzehnder interferometric (MZI) structure and their applications for optical technology, especially in design of all optical switches. In this, we have demonstrated the design and performance of basic MZI switching element (2 × 2 all optical switch) Ti indiffused lithium niobate waveguide, while considering the optimum design parameters. The effect of electrodes shapes and size on the switching driving voltage is also discussed. Application of Lithium Niobate and when doped with Titanium, are discussed. The uses of MZI structures to design all optical switches are reviewed in short and the design of basic 2x2 all optical switch on Ti doped lithium niobate substrate discussed in brief. This work is expected to prove as a useful informative document for current and future researchers to begin with for high end design of Ti indiffused LN based large all optical MZI switches. Losses within the switches have greater impact on their performance, and a detailed investigation on these will add useful suggestion to design better ones. Inclusion of semiconductor amplifiers (SOA's) within or outside these structures has shown enhanced switching characteristics. Ultrafast all-optical signal processing using SOA based symmetric mach-zehnder switch (SMZs) is demonstrated at (Tajima et al., 2001). (Zhujun Wan et al. 2007) reported a fast (response time less then 3ms) 2 × 2 integrated thermo optic Machzehnder interferometer (MZI) switch based on multimode interference (MMI) couplers, with 3.40 dB insertion loss, 0.47 dB polarization dependent loss and extinction ratio (ER) at bar state and cross are 32.01 dB, 16.42 dB respectively. MZI with SOA based tree architecture, have been used to design integrated all optical logic and arithmetic operations. This architecture enables all optical processing of signals, including two input logic operations, half-adder, full-adder, full-subtractor, one-bit data comparator, etc (Roy, 2007).

7. References

Agrawal. N, C. M. Weinert, H.4. Ehrke, G. G. Mekonnen, D. Franke, C. Bornholdt, and R. Langenhorst (1995) "Fast 2 x 2 Mach-Zehnder optical space switches using InGaAsP-InP multiquantum- well structures" IEEE Photonics technology letters, Vol. 7, No. 6, page no. 644-645, June 1995.

Alferness R. C. (1986) "Ti-diffused lithium niobate waveguide devices" ieeexplorer, CH 2358-O/86/0000-0001, 1986.

Arrioja D.A. May, P. LiKamWa, I. Shubin, P.K.L. Yu (2008) "Integrated InGaAsP MQW Mach–Zehnder modulator" Microelectronics Journal, Volume 39, Issues 3-4, March-April 2008, Pages 660-663.

Binh LN, TL Huynh and A. Rahman (2007) "Raman optically amplified MSK multi-span transmission Systems: simulation", © Monash University, 2007.

Gupta S., M. Presi, N. Calabretta, G. Contestabile, E. Ciaramella (2007) "Operational equivalence of self-switching effect in SOA-based nonlinear polarization and MZI switches" ieeexplorer, 1-4244-0925-X, page no. 810-811,2007.

Han Tae Yong, Hyun-Shik Lee and El-Hang Lee (2008) "Design of compact silicon optical modulator using photonic crystal MZI structure" ieeexplorer, page no. 308-310, 978-1-4244-1768-1/2008.

Kalabin Ivan E., Tatiana I. Grigorieva, Lev D. Pokrovsky and Victor V. Atuchin (2004) "High quality double doped polarizing insertion in titanium diffused lithium niobate waveguides" 5th International siberian workshop and tutorial EDM'2004, session I, July 1-5, ERLAGOL, page no. 48-50, ISBN 5-7782-0463-9.

Korkishko Yu.N., V.A. Fedorov, S.M. Kostritskii, A.N. Alkaev, E.I. Maslennikov, E.M. Paderin, D.V. Apraksin, F. Laurell (2003) , Microelectronic Engeneering, 69 (2003) 228-236.

Papadimitriou, Georgios I., Chrisoula Papazoglou, and Andreas S. Pomportsis (2003) "Optical Switching: Switch Fabrics,Techniques, and Architectures" Journal of Lightwave Technology, Vol. 21, No. 2, page no. 384-405, February 2003.

Roy Jitendra Nath (2007) "Mach–Zehnder interferometer-based tree architecture for all-optical logic and arithmetic operations" Optik - International Journal for Light and Electron Optics, In Press, available online 26 November 2007.

Schreieck Roland, Martin Kwakernaak, Heinz Jäckel, Emil Gamper, Emilio Gini, Werner Vogt, Hans Melchior (2001) "Ultrafast Switching Dynamics of Mach–Zehnder Interferometer Switches" IEEE Photonics Technology Letters, Vol. 13, NO. 6, page no. 603-605, JUNE 2001.

Shintaro Niwal, Shinji Matsuo,Takaaki Kakitsuka, Kenichi Kitayama (2008) "Experimental demonstration of 1x4 InP/lnGaAsP optical integrated multimode interference waveguide switch" 20th International Conference on Indium Phosphide and Related Materials, IPRM 2008, Page(s):1 – 4, 25-29 May 2008.

Song Xueliang, Naoki Futakuchi, Foo Cheong Yit, Zhenrui Zhang,Yoshiaki Nakano (2005) "28-ps switching window with a selective area MOVPE all-optical MZI switch" IEEE Photonics Technology Letters, Vol. 17, No. 7, July 2005.

Suzuki Kenya, Takashi Yamada, Osamu Moriwaki, Hiroshi Takahashi and Masayuki Okuno (2008) "Polarization-insensitive MZI switch composed of an in phase shifter array and silica-based plc-integrated polarization beam splitter" OFC/NFOEC 2008, ieeexplore.ieee.org/iel5/4512186/4528018/04528714.

Tajima K. , S. Nakamura and Y. Ueno (2001) "Ultrafast all-optical signal processing with Symmetric Mach–Zehnder type all-optical switches" Optical and Quantum Electronics, Volume 33, Numbers 7-10 / July, 2001.

Thylen, L. (1989) "Lithium Niobate Devices in Switching and Multiplexing" Philosophical Transactions of the Royal Society of London. Series A, Mathematical and Physical Sciences, Volume 329, Issue 1603, pp. 83-92, Sept., 1989.

Toliver P., R. J. Runser, I. Glesk, and P. R. Prucnal (2000) "Comparison of three nonlinear optical switch geometries," in Proc. Conf. on Lasers and Electro-Optics (CLEO 2000), San Francisco, CA, May 7–12, pp.254–255.

Wang T.-J., Chung J.-S. (2004), IEEE photon. Technol. Lett. 16 (2004), 2275.

Wong H. Y., M. Sorel,A. C. Bryce,J. H. Marsh, J. M. Arnold (2005) "Monolithically integrated InGaAs–AlGaInAs Mach–zehnder interferometer optical switch using quantum-well intermixing" IEEE Photonics Technology Letters, Vol. 17, No. 4, page no. 783-785, April 2005.

Wooten Ed L., Karl M. Kissa, Alfredo Yi-Yan, Edmond J. Murphy, Donald A. Lafaw, Peter F. Hallemeier, David Maack, Daniel V. Attanasio, Daniel J. Fritz, Gregory J. McBrien, Donald E. Bossi (2000) "A Review of Lithium Niobate Modulators for Fiber-Optic Communications Systems" IEEE Journal of selected topics in Quantum Electronics, Vol. 6, No. 1, page no. 69-80, January/February 2000.

Xiaobo Hou (2004) "A leaky waveguide all-optical analog-to-digital converter" A PhD thesis, Drexel University, December 2004.

Xiuping Xie (2006) " High gain parametric processes in quasi-phase matching proton-exchange lithium niobate waveguides" Ph.D dissertation, the department of applied physics, Stanford University, September 2006.

Yao Yu Ji, X.S, Maleki L. (1999) " Compact optoelectronic oscillator with ultra-low phase noise performance" electronics letters, 1554, vol. 35, No. 18, 2^{nd} September, 1999.

Zhujun Wan, Yaming Wu, Sihua Li (2007) "Experimental research on an integrated thermo optic switch based on multimode interference couplers" Frontiers of Electrical and Electronic Engineering in China, Volume 2, Number 1, March, 2007.

Authors:

Mr. Ghanshyam Singh. He has completed B.E from REC Silchar (1997), M.Tech from MNIT Jaipur (2003) and is currently pursuing PhD. His areas of interest include Optical Communication, Optical Switches, Optical digital logics & Interconnects.

Prof. R.P.Yadav. He has completed his Master of Science and Master of Technology from IIT Delhi and Ph.D. degree from MNIT Jaipur. He is currently working as the head of Dept. of ECE, MNIT. His areas of interest are Digital and Wireless Communication and Coding, Antennas, Optics and Networking.

Dr. Vijay Janyani. He has completed B.E. and M.E. from MREC Jaipur and PhD from Nottingham University, UK. He is currently working as Asso. Prof., Dept.of ECE, MNIT. His areas of interest include Optoelectronics, Nonlinear Optic and Numerical Modeling.

New Advanced Technologies
Edited by Aleksandar Lazinica

ISBN 978-953-307-067-4
Hard cover, 350 pages
Publisher InTech
Published online 01, March, 2010
Published in print edition March, 2010

This book collects original and innovative research studies concerning advanced technologies in a very wide range of applications. The book is compiled of 22 chapters written by researchers from different areas and different parts of the world. The book will therefore have an international readership of a wide spectrum.